



Synthesis of Functional Ceramic Supports by Ice Templatting and Atomic Layer Deposition

Sylvain Deville, Michaela Klotz, Matthieu Weber, Didier Oison, Igor Iatsunskyi, Emerson Coy, Mikhael Bechelany

► To cite this version:

Sylvain Deville, Michaela Klotz, Matthieu Weber, Didier Oison, Igor Iatsunskyi, et al.. Synthesis of Functional Ceramic Supports by Ice Templatting and Atomic Layer Deposition. *Frontiers in Materials. Computational Materials Science section*, 2018, 5, pp.28. 10.3389/fmats.2018.00028 . hal-01798889

HAL Id: hal-01798889

<https://hal.science/hal-01798889>

Submitted on 24 May 2018

HAL is a multi-disciplinary open access archive for the deposit and dissemination of scientific research documents, whether they are published or not. The documents may come from teaching and research institutions in France or abroad, or from public or private research centers.

L'archive ouverte pluridisciplinaire **HAL**, est destinée au dépôt et à la diffusion de documents scientifiques de niveau recherche, publiés ou non, émanant des établissements d'enseignement et de recherche français ou étrangers, des laboratoires publics ou privés.



Synthesis of Functional Ceramic Supports by Ice Templating and Atomic Layer Deposition

Michaela Klotz^{1*}, Matthieu Weber², Sylvain Deville¹, Didier Oison³, Igor Iatsunskyi⁴, Emerson Coy⁴ and Mikhael Bechelany²

¹ Laboratoire de Synthèse et Fonctionnalisation des Céramiques, UMR3080, Centre National de la Recherche Scientifique/Saint-Gobain CREE, Cavaillon, France, ² Centre National de la Recherche Scientifique, Institut Européen des Membranes, UMR-5635, Université Montpellier, ENSCM - École Nationale Supérieure de Chimie de Montpellier, Montpellier, France, ³ Saint-Gobain CREE, Cavaillon, France, ⁴ NanoBioMedical Centre, Adam Mickiewicz University, Poznan, Poland

OPEN ACCESS

Edited by:

Rajesh Adhikari,
Institut National de la Recherche Scientifique (INRS), Canada

Reviewed by:

Sudip Mondal,
Pukyong National University,
South Korea
Tridib Kumar Sinha,
Gyeongsang National University,
South Korea

*Correspondence:

Michaela Klotz
michaela.klotz@saint-gobain.com

Specialty section:

This article was submitted to
Functional Ceramics,
a section of the journal
Frontiers in Materials

Received: 19 February 2018

Accepted: 23 April 2018

Published: 24 May 2018

Citation:

Klotz M, Weber M, Deville S, Oison D, Iatsunskyi I, Coy E and Bechelany M (2018) Synthesis of Functional Ceramic Supports by Ice Templating and Atomic Layer Deposition. *Front. Mater.* 5:28.
doi: 10.3389/fmats.2018.00028

In this work, we report an innovative route for the manufacturing of functional ceramic supports, by combining ice templating of yttria stabilized zirconia (YSZ) and atomic layer deposition (ALD) of Al_2O_3 processes. Ceramic YSZ monoliths are prepared using the ice-templating process, which is based on the controlled crystallization of water following a thermal gradient. Sublimation of the ice and the sintering of the material reveal the straight micrometer sized pores shaped by the ice crystal growth. The high temperature sintering allows for the ceramic materials to present excellent mechanical strength and porosities of 67%. Next, the conformality benefit of ALD is used to deposit an alumina coating at the surface of the YSZ pores, in order to obtain a functional material. The Al_2O_3 thin films obtained by ALD are 100 nm thick and conformally deposited within the macroporous ceramic supports, as shown by SEM and EDS analysis. Mercury intrusion experiments revealed a reduction of the entrance pore diameter, in line with the growth per cycle of 2 Å of the ALD process. In addition to the manufacture of the innovative ceramic nanomaterials, this article also describes the fine characterization of the coatings obtained using mercury intrusion, SEM and XRD analysis.

Keywords: ice-templating, atomic layer deposition, aluminum oxide, porosity, ceramics

INTRODUCTION

Macroporous ceramic materials are the focus of interest because of their industrial applications, such as catalysis, filtration, and separation, for gas or liquids. These materials have also prospects in the biomedical field, since they could be used to integrate diseased or damaged bone tissues, or for drug delivery applications. Furthermore, hard and functional coating bring more mechanical, thermal, and chemical protection (Zhang and Lawn, 2004). In applications where the transport of matter is the limiting factor, the use of oriented macroporosity is highly desired. When compared to the classical extrusion processes, ice-templating appears as a particularly interesting manufacturing process, as it extends the range of accessible macropore size down to a few microns (Nishihara et al., 2005; Deville et al., 2011; Zhou et al., 2011; Deville, 2013, 2017). The process basically consists of freezing a suspension, followed by the sublimation of the frozen phase and subsequent sintering. A porous structure with unidirectional channels is obtained in the case of unidirectional freezing. The pores are a replica of the solvent (water in our case) crystals (Deville, 2013, 2017). Depending on the chosen application, the obtained macropore surface needs to be decorated with active sites

in order to obtain a functional material. Aluminum oxide (Al_2O_3) thin films have attracted a lot of attention due to their potential applications in diverse areas, from microelectronics (Groner et al., 2002) to catalysis (Cejka, 2003). Due to the fact that macroporous materials have low specific surface area, in order to disperse and anchor active sites, the ceramic material surface is typically covered by a thin porous layer using a washcoating process. However, the desired reduction of the macropore diameter for certain applications comes with technical issues regarding the washcoating processes. In fact, conventional liquid methods are no longer suitable, because capillary forces prevent homogeneous drying of the washcoat, leading to the undesired clogging of the pores.

Atomic layer deposition (ALD) is a vacuum deposition technology, currently considered as the method of choice to deposit conformal ultrathin films of a wide variety of materials for a growing number of applications (Leskelä and Ritala, 2003; George, 2010; Marichy et al., 2012; Hamalainen et al., 2014; Weber et al., 2015, 2017; Pavlenko et al., 2016; Hirsch et al., 2017). Due to the self-limiting surface chemistry taking place during the alternating precursor and co-reactant pulses, each ALD cycle results in the deposition of a (sub) monolayer of atoms, and the growth of the thin film is thus controllable at the (sub) nanolevel (George, 2010). Apart of the atomic control over the film thickness, the self-limiting half-cycles in ALD enables to obtain uniform depositions over large substrates as well as conformal depositions in structures presenting high aspect ratio and complex 3D structures (Ritala et al., 1999; Leskelä and Ritala, 2002, 2003). ALD of Al_2O_3 is the most used and studied ALD process, and it can be considered as a typical and “close-to-ideal” ALD process (Berland et al., 1998; Ritala et al., 1999; Leskelä and Ritala, 2002, 2003; George, 2010). In the past, ultrathin layers of Al_2O_3 were deposited conformally onto various substrates, such as nanopores or carbon fibers for example (Ott et al., 1997; Roy et al., 2010).

The present study describes a novel route for the preparation of functional ceramics, combining the ice templating process of yttria stabilized zirconia (YSZ) with an ALD of alumina process. YSZ is an attractive material and has important industrial applications, thanks to its chemical and thermal stability, as well as its oxygen ion conductivity. We report the successful deposition of a 100 nm film conformally covering the inner pores of ice templated YSZ, and we present the fine characterization of the materials obtained. The novel process described and the results presented open prospects for filtration and catalysis applications.

MATERIALS AND METHODS

Ice-templated monoliths of 3 mol% YSZ were prepared from aqueous ceramic slurry, following a procedure described previously (Seuba et al., 2016). Briefly, the aqueous slurry was prepared with 3 mol% YSZ (TZ-3YS, Tosoh, Japan), and 10 ml of the slurry was then poured into a PTFE mold (20 mm diameter and 25 mm height) placed on a copper plate. The sample was frozen from the bottom by circulating silicone oil regulated

by a cryothermostat (Model CC905, Hubert) underneath the copper plate with a cooling rate of 2°C/min, whereas the temperature of the top of the sample remained exposed to air. After solidification, samples were removed from the molds and ice was sublimated for at least 48 h using a commercial freeze-dryer (Free Zone 2.5 Plus, Labconco, Kansas City, Missouri, USA) and then sintered at 3°C/min rate up to an intermediate dwell at 500°C for 3 h to remove the binder and then at 5°C/min up to 1,300°C for 3 h. The top and bottom of the monoliths were cut using a diamond saw for a final monolith height of 1 cm.

All ALD experiments were carried out in a home-built cross-flow reactor, described elsewhere (Whitby et al., 2012; Viter et al., 2016). The ALD of Al_2O_3 process was based on trimethylaluminum [TMA, $\text{Al}(\text{CH}_3)_3$] as precursor and water as co-reactant at a deposition temperature of 100°C. The TMA precursor purchased was placed in a stainless steel bubbler under Ar in a glovebox, sealed carefully, and then directly connected to the inlet of a pneumatic valve, and metal gaskets were employed for seal fittings to the ALD reactor, therefore limiting the risks associated with this pyrophoric precursor. Briefly, the process consisted of 0.1 s pulse TMA, 30 s exposure, 40 s purge with Argon, 2 s water pulse, 30 s exposure 40 s purge with Argon to finish the cycle. If not specified otherwise, 500 cycles have been used to prepare the alumina films. Please note that the ALD process has first been studied on Si samples, where the thickness could easily be measured using spectroscopic ellipsometry (Semilab GES5E) (Baitimirova et al., 2016). Following the ALD, some of the samples were thermally treated at 1,150°C at a heating rate of 5°C/min with a dwell at this temperature for 1 or 10 h, depending on the samples.

Scanning electron microscopy (SEM) has been performed using a Nova NanoSEM 230 (FEI, Hillsboro, USA) on cross-section (fractured) samples and on resin embedded and polished samples. Mercury intrusion porosimetry experiments were carried out using an AutoPore IV 9500 (Micromeritics), pore diameter was calculated using the well-known Washburn equation. The microstructure and the phase of the films were determined by grazing incidence X-ray diffraction (GIXRD) using a Panalytical X'pert 3 system. GIXRD angles of <5 degrees were used in our measurements.

RESULTS AND DISCUSSION

First, templated monoliths of 3 mol% YSZ were prepared following the ice-templating process described previously (Seuba et al., 2016). The unidirectional freezing of water taking place during the ice-templating process enables to obtain regular macroporous materials. The porosity of the sample is correlated to the water concentration, as a first order parameter to the solid loading of the suspension (Deville et al., 2015). The ceramic slurry was placed in a mold, in direct contact with a cold plate. The constant temperature decrease of the cold plate led to the nucleation of ice crystals, which then grew toward the top following the thermal gradient. The monoliths synthesized presented micrometer sized macropores, crossing the sample from bottom to top. The macroporous YSZ monoliths were

characterized using *ex situ* SEM measurements. The sublimation of the ice and the sintering of the green body led to monoliths with oriented macropores of 5 μm diameter, as shown in the SEM

image depicted in **Figure 1A**. The corresponding porosity, in terms of empty space percentage, was around 67%. The close-up view of a fractured wall reveals internal porosity (**Figure 1B**).

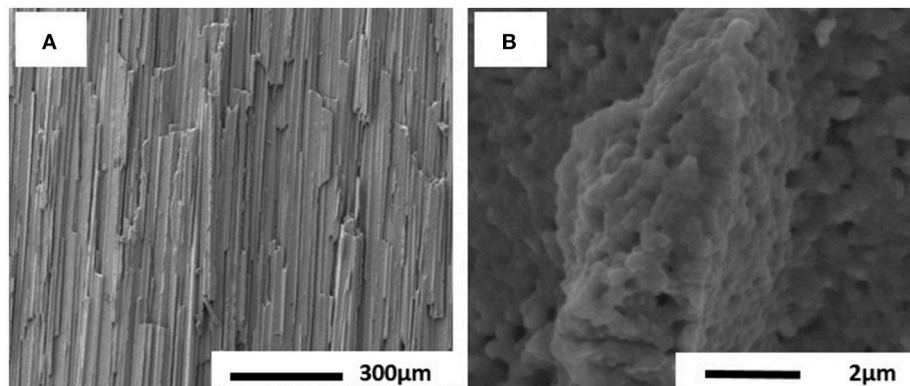


FIGURE 1 | SEM images of fractured sintered YSZ monolith showing **(A)** the oriented macroporosity aligned parallelly to the freezing direction **(B)** a close-up view of the sample.

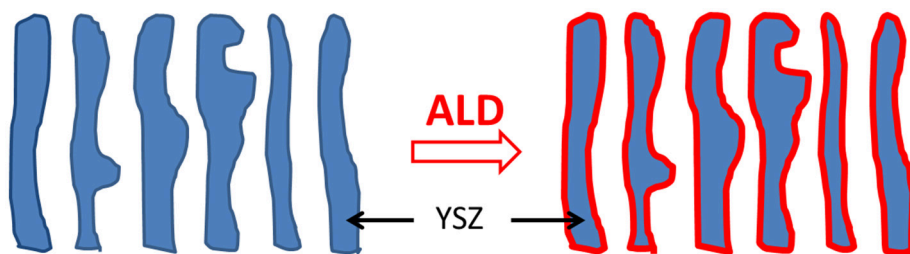


FIGURE 2 | Schematic illustration of the conformal ALD coating of the sintered YSZ substrates (the ALD coating is represented in red color).

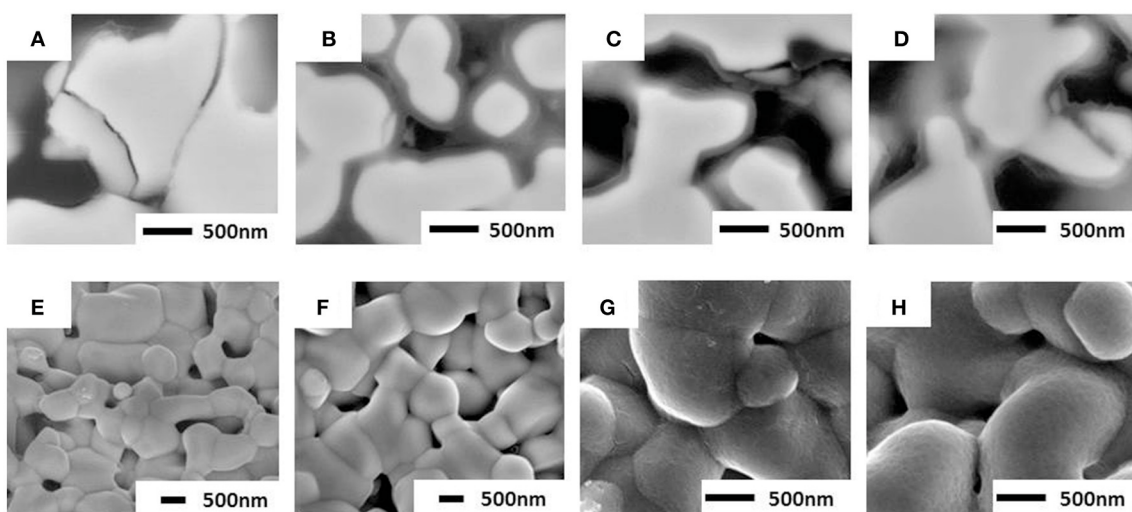


FIGURE 3 | SEM images of **(A,E)** YSZ substrate, **(B,F)** as-deposited ALD coating, **(C,G)** after 1 h at 1,150°C, **(D,H)** after 10 h at 1,150°C. The images presented in **(A–D)** show resin impregnated and polished samples, evidencing the 100 nm thick ALD coating (using a backscattered electron detector). The images shown in **(E–H)** correspond to the fractured samples, showing the surface morphology of the ALD coating and illustrating its conformality.

The YSZ macroporous materials substrates prepared were then coated by ALD. Using 500 cycles of an ALD process based on trimethylaluminum (TMA, Al(CH₃)₃) as precursor and water as co-reactant at a deposition temperature of 100°C, thin films of 100 nm have been prepared. The growth per cycle (GPC) of 2 Å/cycle obtained is in line with previous studies (Viter et al., 2016). The as-deposited coating corresponds to the amorphous phase of Al₂O₃. Thus, thermal treatments at 1,150°C for either 1 or 10 h have been carried out to modify the amorphous phase into crystalline alumina. In order to depict the result of the ALD coating, **Figure 2** presents a schematic illustration of the conformal ALD coating of the sintered YSZ substrate. The

characterization of the coating within the porosity of the ice-templated substrates has then been carried out. The presence of the alumina coating was first revealed using mercury intrusion experiments. A decrease of the macropore diameter by 0.2 μm is clearly visible, which is directly correlated to the 100 nm thick coating on the pore surface. The macropore diameter remains constant regardless of the thermal treatments at 1,150°C. The decrease in pore diameter is in line with the GPC of 2 Å/cycle of the ALD process. However, as the mercury intrusion was made on entire materials, this result characterizes the pore entrance at the surface of the ceramic piece and may not be representative of a homogeneous and conformal coating in the whole material.

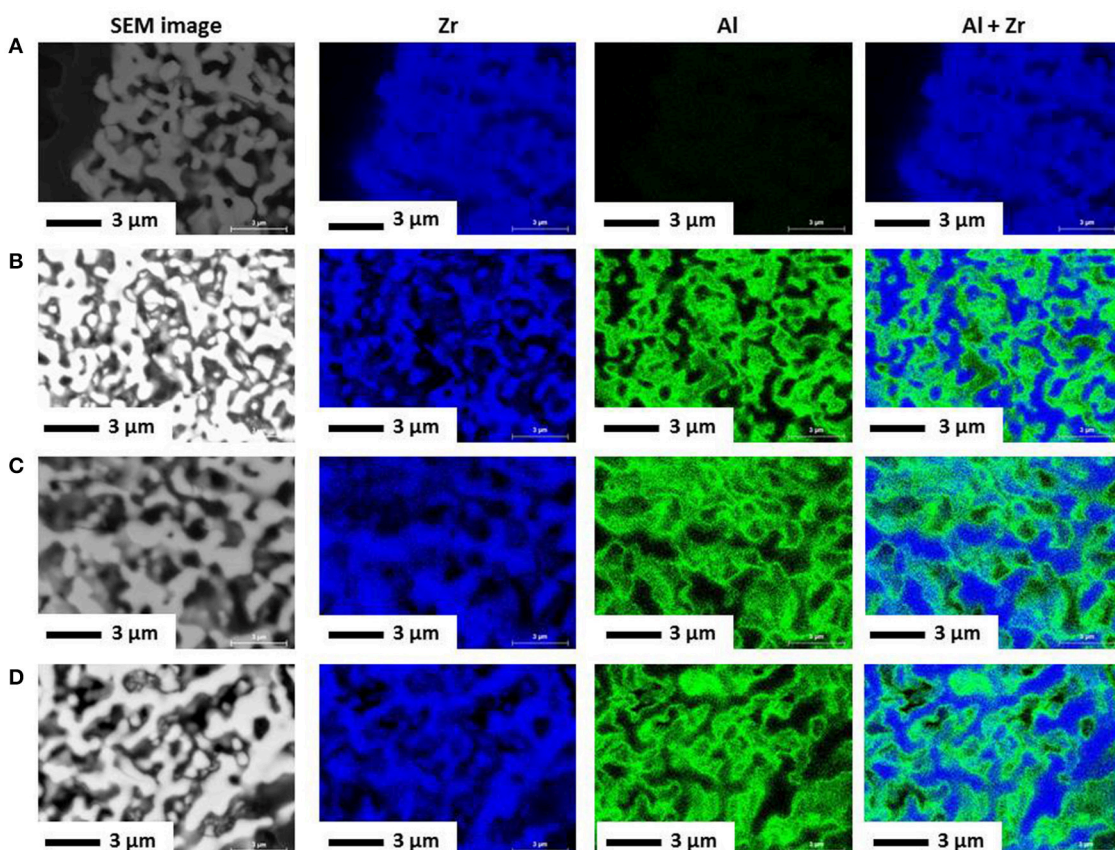
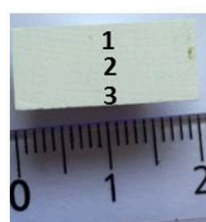


FIGURE 4 | SEM images and EDS mapping of Zr and Al for the **(A)** YSZ substrate **(B)** as-deposited ALD coating **(C)** after 1 h at 1,150°C **(D)** after 10 h at 1,150°C.



Position	1	2	3
Element	Atomic %	Atomic %	Atomic %
O	74	73	69
Al	7	7	9
Zr	19	21	22
Total:	100	100	100

FIGURE 5 | Image of ALD coated monolith cut in half and EDS probe positions 1, 2, and 3 indicated on the image showing homogeneous Al repartition throughout the YSZ monolith.

Thus, in order to verify the homogeneity and the conformality of the films prepared by ALD throughout the entire substrates, SEM studies have been performed on cross sections of the substrates, after resin impregnation and polishing. **Figures 3A–D** depicts representative SEM images of cross sections of the samples cut in their center. To evidence the coatings, the acquisition was made with a vCD backscattered electron detector providing topographical and compositional contrast. The substrate, shown in **Figures 3A,E**, is composed of sintered YSZ grains appearing in light gray in the images. The lighter amorphous alumina ALD is clearly visible in dark gray in **Figure 3B**. The thickness of the coating is ~ 100 nm, in accordance with the pore size decrease measured by mercury intrusion. The thermal treatment at $1,150^{\circ}\text{C}$ (**Figures 3C,D**) does not impact coating thickness. This was confirmed with EDS mapping of the elements Zr and Al, as shown on **Figure 4** on a $14\ \mu\text{m}$ by $10\ \mu\text{m}$ surface. The Zr distribution, shown in blue, overlaps the YSZ grains, in light gray on the corresponding SEM images. The Al contribution is shown in green. No signal is visible for the YSZ substrate, shown by a black signal. For the ALD samples, an Al signal is visible. In comparison with the SEM image, the Al is concentrated in the resin filled pores that appear dark on the SEM image. The Al signal is intense at the YSZ grain surface, where the coating is at the sample surface. Less intense Al signal on the pores is relative to the coating of a grain covered by resin, beneath the sample surface. Furthermore, the repartition of the Al in the whole substrate was checked on a monolith cut in its center (**Figure 5**) and analyzed by EDS at several positions throughout the sample height. The atomic % of Al is constant throughout the samples, depicting nicely the conformality benefit of ALD.

Previous studies of ALD Al_2O_3 films showed correlated changes in structural properties with thermal treatment. As-deposited films are smooth, amorphous and consist of aluminum and oxygen, as well as carbon and hydrogen (Jakschik et al., 2003). As shown in **Figure 3F**, the as-deposited coatings appear dense and smooth. Previous studies have shown that $1,150^{\circ}\text{C}$ is the optimal transition temperature to turn Al_2O_3 thin film from an amorphous phase to a crystalline phase (Zhang et al., 2007). Therefore, thermal treatments at $1,150^{\circ}\text{C}$ for 1 and 10 h have been applied to the coated samples in order to transform the coatings into crystalline alumina.

SEM images (**Figures 3G,H**) show that the thermal treatment modified the aspect of the coating, which appeared to become granular after the treatments at $1,150^{\circ}\text{C}$. No delamination of the coating has been observed. In order to control the crystallinity of the samples, grazing incidence X-ray diffraction has been performed. This technique is particularly suited for very thin films and allows us to determine the phase at the near-surface layers. **Figure 6** compares the pattern respectively of the as-deposited monolith and after the thermal treatment at $1,150^{\circ}\text{C}$. Large level of background scattering is due to the fact that the surface of the monolith is not smooth. The main diffraction peaks are attributed to the tetragonal YSZ and can be indexed with the JC-PDF pattern 04-005-4479. After the thermal treatment, additional peaks relative to hexagonal alpha-Alumina are observed. The alpha alumina crystalline phase

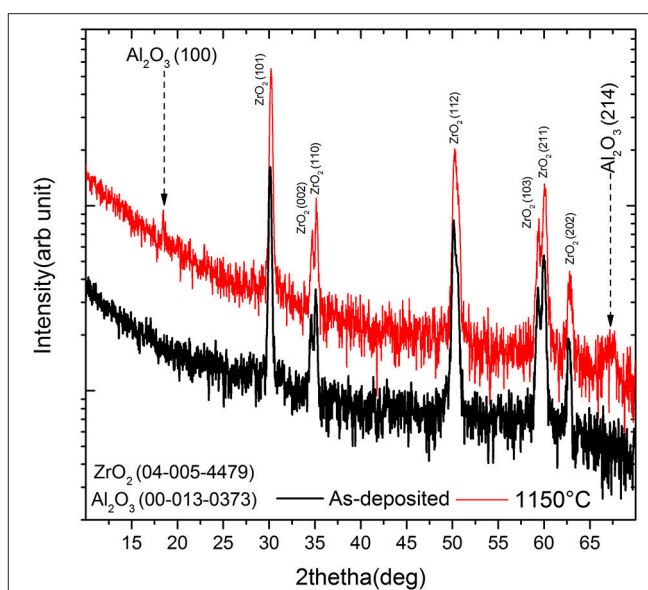


FIGURE 6 | GI-XRD of $1,150^{\circ}\text{C}$ thermally treated YSZ monolith showing low intensity Al_2O_3 peaks after the heat treatment (red pattern), as compared to the pattern of the as-deposited sample (black pattern).

obtained is in line with the thermal treatment carried out at $1,150^{\circ}\text{C}$. Interestingly, it has been shown that annealing ALD Al_2O_3 films above crystallization temperatures increases their dielectric constant, since granular films have a better ability to be polarized. This was attributed to densification and a change in the composition of the film (Jakschik et al., 2003).

CONCLUSION

The present work showed the successful combination of ice-templating and ALD processes for the preparation of functional ceramic materials. Ice-templating is a manufacturing method that is particularly suited to prepare materials with controlled and oriented macroporosity. In this study, templated monoliths of 3 mol% YSZ with controlled macroporosities have been synthesized. To counter the difficulty of depositing a homogeneous coating in the small pores of the ice-templated materials encountered with conventional techniques, we used the ALD route. An ALD process based on TMA and H_2O has been used, and this thin film deposition technique enabled to achieve the conformal deposition of thin films within the pores. Mercury intrusion experiments revealed a decrease of the macropore diameter after ALD corresponding to the deposited thickness. SEM and EDX experiments have shown that a continuous and homogeneous coating was achieved throughout the entire YSZ substrates. Moreover, a thermal treatment at $1,150^{\circ}\text{C}$ has been used to convert the amorphous alumina to its crystalline phase, as demonstrated by grazing incidence XRD.

These proof-of-concept results enabled to show the successful preparation of functional materials, by combining ice-templating and ALD processes. The innovative and versatile route, enabling

the manufacturing of functional macroporous materials, opens prospects for many applications in the fields of catalysis, filtration and biomedicine.

AUTHOR CONTRIBUTIONS

MK, SD, and MB designed and conducted the research project. MK and SD worked on the ice-templating, MB and MW on the ALD. DO, EC, and II made the SEM and GI-XRD analysis. All

authors reviewed and discussed the results, MK and MW wrote the paper.

ACKNOWLEDGMENTS

Jordi Seuba is acknowledged for the preparation of the YSZ monoliths. This work was partly supported by the French Research Program ANR BONALD (ANR-14-CE07-0011) and ANR MeNiNA (ANR-17-CE09-0049).

REFERENCES

- Baitimirova, M., Viter, R., Andzane, J., Van Der Lee, A., Voiry, D., Iatsunskyi, I., et al. (2016). Tuning of structural and optical properties of Graphene/ZnO nanolaminates. *J. Phys. Chem. C* 120, 23716–23725. doi: 10.1021/acs.jpcc.6b07221
- Berland, B. S., Gartland, I. P., Ott, A. W., and George, S. M. (1998). *In situ* monitoring of atomic layer controlled pore reduction in alumina tubular membranes using sequential surface reactions. *Chem. Mater.* 10, 3941–3950. doi: 10.1021/cm980384g
- Cejka, J. (2003). Organized mesoporous alumina: synthesis, structure and potential in catalysis. *Appl. Catalysis A* 254, 327–338. doi: 10.1016/S0926-860X(03)00478-2
- Deville, S. (2013). Ice-templating, freeze casting: beyond materials processing. *J. Mater. Res.* 28, 2202–2219. doi: 10.1557/jmr.2013.105
- Deville, S. (2017). *Freezing Colloids: Observations, Principles, Control, and Use: Applications in Materials Science, Life Science, Earth Science, Food Science, and Engineering*. Cham: Springer International Publishing.
- Deville, S., Meille, S., and Seuba, J. (2015). A meta-analysis of the mechanical properties of ice-templated ceramics and metals. *Sci. Tech. Adv. Mater.* 16:043501. doi: 10.1088/1468-6996/16/4/043501
- Deville, S., Viazzi, C., Leloup, J., Lasalle, A., Guizard, C., Maire, E., et al. (2011). Ice shaping properties, similar to that of antifreeze proteins, of a zirconium acetate complex. *PLoS ONE* 6:e26474. doi: 10.1371/journal.pone.0026474
- George, S. M. (2010). Atomic layer deposition: an overview. *Chem. Rev.* 110, 111–131. doi: 10.1021/cr900056b
- Groner, M., Elam, J., Fabreguette, F., and George, S. M. (2002). Electrical characterization of thin Al₂O₃ films grown by atomic layer deposition on silicon and various metal substrates. *Thin Solid Films* 413, 186–197. doi: 10.1016/S0040-6090(02)00438-8
- Hamalainen, J., Ritala, M., and Leskela, M. (2014). Atomic layer deposition of noble metals and their oxides. *Chem. Mater.* 26, 786–801. doi: 10.1021/cm402221y
- Hirsch, M., Majchrowicz, D., Wierzba, P., Weber, M., Bechelany, M., and Jedrzejewska-Szczerbska, M. (2017). Low-coherence interferometric fiber-optic sensors with potential applications as biosensors. *Sensors* 17:261. doi: 10.3390/s17020261
- Jakschik, S., Schroeder, U., Hecht, T., Gutsche, M., Seidl, H., and Bartha, J. W. (2003). Crystallization behavior of thin ALD-Al 2 O 3 films. *Thin Solid Films* 425, 216–220. doi: 10.1016/S0040-6090(02)01262-2
- Leskelä, M., and Ritala, M. (2002). Atomic layer deposition (ALD): from precursors to thin film structures. *Thin Solid Films* 409, 138–146. doi: 10.1016/S0040-6090(02)00117-7
- Leskelä, M., and Ritala, M. (2003). Atomic layer deposition chemistry: recent developments and future challenges. *Angew. Chem. Int. Ed.* 42, 5548–5554. doi: 10.1002/anie.200301652
- Marichy, C., Bechelany, M., and Pinna, N. (2012). Atomic layer deposition of nanostructured materials for energy and environmental applications. *Adv. Mater.* 24, 1017–1032. doi: 10.1002/adma.201104129
- Nishihara, H., Mukai, S. R., Yamashita, D., and Tamon, H. (2005). Ordered macroporous silica by ice templating. *Chem. Mater.* 17, 683–689. doi: 10.1021/cm048725f
- Ott, A., Klaus, J., Johnson, J., George, S., McCarley, K., and Way, J. (1997). Modification of porous alumina membranes using Al₂O₃ atomic layer controlled deposition. *Chem. Mater.* 9, 707–714. doi: 10.1021/cm960377x
- Pavlenko, M., Coy, E., Jancelewicz, M., Zaleski, K., Smyntyna, V., Jurga, S., et al. (2016). Enhancement of optical and mechanical properties of Si nanopillars by ALD TiO 2 coating. *RSC Adv.* 6, 97070–97076. doi: 10.1039/C6RA21742G
- Ritala, M., Leskela, M., Dekker, J.-P., Mutsaers, C., Soininen, P. J., and Skarp, J. (1999). Perfectly conformal TiN and Al₂O₃ films deposited by atomic layer deposition. *Chem. Vap. Depos.* 5, 7–9. doi: 10.1002/(SICI)1521-3862(199901)5:1<7::AID-CVDE7>3.0.CO;2-J
- Roy, A., Baumann, W., König, I., Baumann, G., Schulze, S., Hietschold, M., et al. (2010). Atomic layer deposition (ALD) as a coating tool for reinforcing fibers. *Anal. Bioanal. Chem.* 396, 1913–1919. doi: 10.1007/s00216-010-3470-9
- Seuba, J., Deville, S., Guizard, C., and Stevenson, A. J. (2016). The effect of wall thickness distribution on mechanical reliability and strength in unidirectional porous ceramics. *Sci. Techn. Adv. Mater.* 17, 128–135. doi: 10.1080/14686996.2016.1140309
- Viter, R., Iatsunskyi, I., Fedorenko, V., Tumenas, S., Balevicius, Z., Ramanavicius, A., et al. (2016). Enhancement of electronic and optical properties of ZnO/Al₂O₃ nanolaminate coated electrospun nanofibers. *J. Phys. Chem. C* 120, 5124–5132. doi: 10.1021/acs.jpcc.5b12263
- Weber, M. J., Verheijen, M. A., Bol, A. A., and Kessels, W. M. M. (2015). Sub-nanometer dimensions control of core/shell nanoparticles prepared by atomic layer deposition. *Nanotechnology* 26:094002. doi: 10.1088/0957-4484/26/9/094002
- Weber, M., Koonkaew, B., Balme, S., Utke, I., Picaud, F., Iatsunskyi, I., et al. (2017). Boron nitride nanoporous membranes with high surface charge by atomic layer deposition. *ACS Appl. Mater. Interfaces* 9, 16669–16678. doi: 10.1021/acsm.7b02883
- Whitby, J. A., Ostlund, F., Horvath, P., Gabureac, M., Riesterer, J. L., Utke, I., et al. (2012). High spatial resolution time-of-flight secondary ion mass spectrometry for the masses: a novel orthogonal ToF FIB-SIMS instrument with *in situ* AFM. *Adv. Mater. Sci. Eng.* 2012:180437. doi: 10.1155/2012/180437
- Zhang, L., Jiang, H., Liu, C., Dong, J., and Chow, P. (2007). Annealing of Al₂O₃ thin films prepared by atomic layer deposition. *J. Phys. D Appl. Phys.* 40, 3707. doi: 10.1088/0022-3727/40/12/025
- Zhang, Y., and Lawn, B. (2004). Long-term strength of ceramics for biomedical applications. *J. Biomed. Mater. Part B Appl. Biomater.* 69B, 166–172. doi: 10.1002/jbm.b.20039
- Zhou, K., Zhang, Y., Zhang, D., Zhang, X., Li, Z., Liu, G., et al. (2011). Porous hydroxyapatite ceramics fabricated by an ice-templating method. *Scr. Mater.* 64, 426–429. doi: 10.1016/j.scriptamat.2010.11.001

Conflict of Interest Statement: The authors declare that the research was conducted in the absence of any commercial or financial relationships that could be construed as a potential conflict of interest.

Copyright © 2018 Klotz, Weber, Deville, Oison, Iatsunskyi, Coy and Bechelany. This is an open-access article distributed under the terms of the Creative Commons Attribution License (CC BY). The use, distribution or reproduction in other forums is permitted, provided the original author(s) and the copyright owner are credited and that the original publication in this journal is cited, in accordance with accepted academic practice. No use, distribution or reproduction is permitted which does not comply with these terms.